Virology 407 (2010) 213–224

Contents lists available at ScienceDirect

Virology

journal homepage: www.elsevier.com/locate/yviro

Interactions between p27 and p88 replicase proteins of *Red clover necrotic mosaic virus* play an essential role in viral RNA replication and suppression of RNA silencing via the 480-kDa viral replicase complex assembly

Akira Mine, Kiwamu Hyodo, Atsushi Takeda [1], Masanori Kaido, Kazuyuki Mise, Tetsuro Okuno *

Laboratory of Plant Pathology, Graduate School of Agriculture, Kyoto University, Sakyo-ku, Kyoto 606-8502, Japan

ARTICLE INFO

Article history:
Received 9 June 2010
Returned to author for revision 13 July 2010
Accepted 23 July 2010
Available online 15 September 2010

Keywords:
Positive-sense RNA virus
Viral RNA replication
Viral replicase complex
Protein–protein interaction
Coimmunoprecipitation analysis
Blue-native PAGE
Dianthovirus
Tombusviridae
RNA-dependent RNA polymerase
RNA silencing suppression
In vitro translation and RNA synthesis

ABSTRACT

Red clover necrotic mosaic virus (RCNMV), a positive-sense RNA virus with a bipartite genome, encodes p27 and p88 replicase proteins that are required for viral RNA replication and suppression of RNA silencing. In this study, we indentified domains in p27 and p88 responsible for their protein–protein interactions using *in vitro* pull-down assays with the purified recombinant proteins. Coimmunoprecipitation analysis in combination with blue-native polyacrylamide gel electrophoresis using mutated p27 proteins showed that both p27–p27 and p27–p88 interactions are essential for the formation of the 480-kDa complex, which has RCNMV-specific RNA-dependent RNA polymerase activity. Furthermore, we found a good correlation between the accumulated levels of the 480-kDa complex and replication levels and the suppression of RNA silencing activity. Our results indicate that interactions between RCNMV replicase proteins play an essential role in viral RNA replication and in suppressing RNA silencing via the 480-kDa replicase complex assembly.

Introduction

The viral replicase complexes of positive-sense RNA viruses of eukaryotes contain viral RNA templates, viral replicase proteins and host proteins, which are assembled on intracellular membranes in infected cells (Ahlquist et al., 2003). Previous studies have revealed that the assembly of functional viral replicase complexes requires interactions between viral replicase proteins. For instance, the *Tomato bushy stunt virus* (TBSV)-encoded p33 replicase protein interacts with other p33 replicase proteins *in vivo* and *in vitro* and also interacts with another TBSV-encoded replicase protein, p92, containing an RNA-dependent RNA polymerase (RdRP) motif (Rajendran and Nagy, 2004, 2006). Coimmunoprecipitation analysis and replication studies have demonstrated that an interaction between p33 and p92 is required for the assembly of the TBSV replicase complex in yeast, a model host for TBSV replication study (Rajendran and Nagy, 2006). Other examples are the N-terminally overlapping 126K and 183K replicase proteins of *Tobacco mosaic virus* (TMV). These proteins interact through their helicase domains in the overlapping region (Goregaoker et al., 2001; Watanabe et al., 1999). This is essential for TMV replication (Goregaoker et al., 2001; Goregaoker and Culver, 2003). In *Brome mosaic virus* (BMV), the 1a replicase protein interacts with other 1a proteins, and also interacts with the 2a replicase protein containing RdRP motif (Kao and Ahlquist, 1992; Kao et al., 1992; O'Reilly et al., 1995, 1997, 1998). Interaction between 1a and 2a is essential for BMV replication (O'Reilly et al., 1998). Functional interactions between viral replicase proteins have also been reported for other positive-sense RNA viruses, including *Flock house virus* (Dye et al., 2005), poliovirus (Hope et al., 1997; Hobson et al., 2001; Strauss and Wuttke, 2007), and hepatitis C virus (HCV) (Qin et al., 2002; Wang et al., 2002).

Red clover necrotic mosaic virus (RCNMV) is a positive-sense single-stranded RNA plant virus and a member of the genus *Dianthovirus* in the family *Tombusviridae*. Its genome is divided into RNA1 and RNA2, which both have no cap structure at the 5′ end (Mizumoto et al., 2003) and no poly(A) tail at the 3′ end (Lommel et al., 1988; Mizumoto et al., 2003; Xiong and Lommel, 1989).

RNA1 encodes N-terminally overlapping replicase proteins of 27 kDa (p27) and 88 kDa (p88). Of these, p88 contains an RdRP motif

* Corresponding author. Laboratory of Plant Pathology, Graduate School of Agriculture, Kyoto University, Sakyo-ku, Kitashirakawa, Kyoto 606-8502, Japan. Fax: +81 75 753 6131.
E-mail address: okuno@kais.kyoto-u.ac.jp (T. Okuno).
[1] Present address: Department of Life Sciences, Graduate School of Arts and Sciences, The University of Tokyo, Komaba 3-8-1, Meguro-ku, Tokyo 153-8902, Japan.

0042-6822/$ – see front matter © 2010 Elsevier Inc. All rights reserved.
doi:10.1016/j.virol.2010.07.038

(Koonin, 1991), is translated via a programmed −1 ribosomal frameshifting (Xiong et al., 1993; Kim and Lommel, 1994), and is required in *cis* for the replication of RNA1 (Okamoto et al., 2008). Both p27 and p88 are present in a purified RCNMV RdRP fraction (Bates et al., 1995; Mine et al., 2010). Our previous study has demonstrated that: (i) p27 and p88 form tightly membrane-associated protein complexes with apparent molecular masses of 380 kDa and 480 kDa, possibly through p27–p27 and p27–p88 interactions; (ii) the 380-kDa complex contains only p27 as a virus-derived component, whereas the 480-kDa complex contains both p27 and p88; and (iii) the 480-kDa complex retains RdRP activity that synthesizes RNA fragments by recognizing the core promoter sequences at the 3′ termini of RCNMV RNAs *in vitro* (Mine et al., 2010). In addition, both p27 and p88 together with viral RNAs competent for negative-strand RNA synthesis are required for the suppression of RNA silencing (Takeda et al., 2005). Furthermore, the cap-independent translational activity of RNA2 is linked strongly to the replication of RNA2 (Mizumoto et al., 2006). This is in contrast to that of RNA1, which contains a cap-independent translation enhancer, named 3′TE-DR1 in the 3′ untranslated region (Mizumoto et al., 2003). These studies suggested that interactions between p27 and p88 play important roles in RCNMV infection processes including formation of the 480-kDa complex, viral RNA replication, suppression of RNA silencing, and possibly cap-independent translation of RNA2. However, the roles of p27–p27 and p27–p88 interactions in these processes have not been elucidated.

In this study, we investigated the interactions between RCNMV replicase proteins, p27 with p27, p27 with p88 and the roles of these interactions in the formation of the 480-kDa complex, viral RNA replication and suppression of RNA silencing. Glutathione-S-transferase (GST) pull-down assays using purified recombinant p27 and p88 revealed that p27 interacts with both p27 and p88 through direct protein–protein contacts, and that the C-terminal half of p27 is responsible for these interactions, whereas the non-overlapping region unique to p88 is responsible for p27–p88 interaction. We also found that both p27–p27 and p27–p88 interactions are required for the formation of the 480-kDa complex, and that there were good correlations between the accumulated levels of the 480-kDa complex and replication levels and suppression of RNA silencing activity. Overall, our study supplies strong evidence that interactions between p27 and p88 replicase proteins play an essential role in RCNMV RNA replication and suppression of RNA silencing via the 480-kDa viral replicase complex assembly.

Results

In vitro protein–protein interactions between RCNMV replicase proteins

To test whether p27–p27 and p27–p88 interactions occur through protein–protein contacts, we performed an *in vitro* GST pull-down assay. For this assay, we expressed p27 containing an N-terminal His-tag and a C-terminal FLAG-tag (His-p27-FLAG) in *Escherichia coli* and purified it as described in the Materials and methods (Fig. 1A). We also expressed N-terminally His- and GST-fused p27 (His/GST-p27) and p88 (His/GST-p88) in *E. coli*. His/GST-p27 and His/GST-p88 captured on glutathione-bound beads were incubated with purified His-p27-FLAG. After extensive washing, the bound proteins were analyzed by western blotting with an anti-FLAG antibody. His-p27-FLAG was efficiently pulled down by His/GST-p27 and His/GST-p88, but not by His/GST, used as a negative control (Fig. 1B). These results indicate that p27 can interact with both p27 and p88 through protein–protein contacts.

Domains in p27 responsible for p27–p27 and p27–p88 interactions

To determine the domains in p27 responsible for p27–p27 interaction, first we tested interactions of His-p27-FLAG with the His/GST-fused N-terminal half of p27 (His/GST-p27N) or C-terminal half of p27 (His/GST-p27C) using an *in vitro* pull-down assay. The N-terminal half and the C-terminal half of p27 consist of amino acid sequences 1–113 and 114–236, respectively (Fig. 2A). His-p27-FLAG was recovered efficiently by His/GST-p27C, but not as much by His/GST-p27N (Fig. 2B). These results suggest that the C-terminal half of p27 is mainly involved in p27–p27 interaction.

To confirm that p27–p27 interaction is directed through contacts between the C-terminal half of p27, we tested interactions of His/GST-p27C with two truncated versions of His-p27-FLAG (His-p27N-FLAG and His-p27C-FLAG). His-p27N-FLAG and His-p27C-FLAG contain the N-terminal half or the C-terminal half of p27, respectively (Figs. 2A and C). GST pull-down assays showed that His-p27N-FLAG

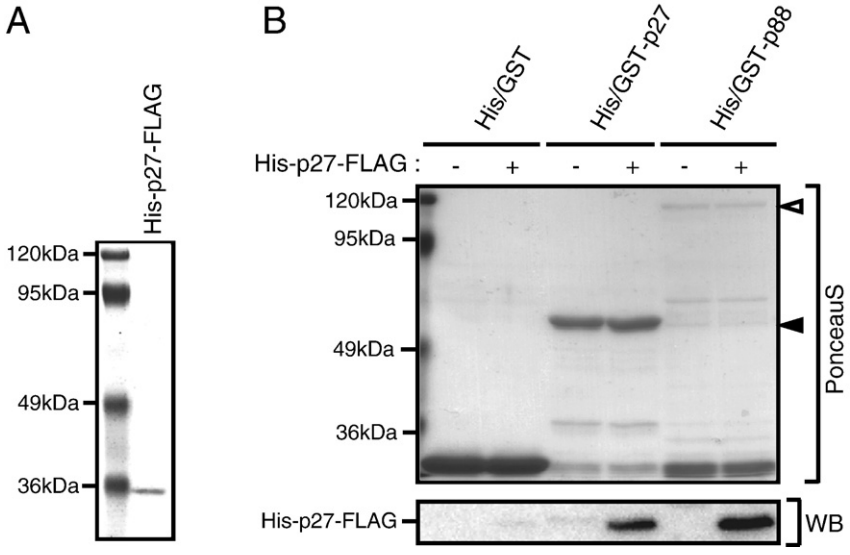

Fig. 1. *In vitro* protein–protein interactions between RCNMV replicase proteins. (A) SDS-PAGE analysis of purified His-p27-FLAG expressed in *E. coli*. The purified protein (500 ng) was visualized with CBB staining. (B) GST pull-down analysis of p27–p27 and p27–p88 interactions. Glutathione resin-bound His/GST-fused p27 or p88 proteins were incubated with the purified His-p27-FLAG. After washing, pulled-down complexes were subjected to SDS-PAGE and blotted onto a membrane. The separated proteins on the membrane were visualized with PonceauS staining (PonceauS), and analyzed by western blotting using anti-FLAG antibody (WB). Black and white arrowheads, respectively, indicate His/GST-p27 and His/GST-p88.

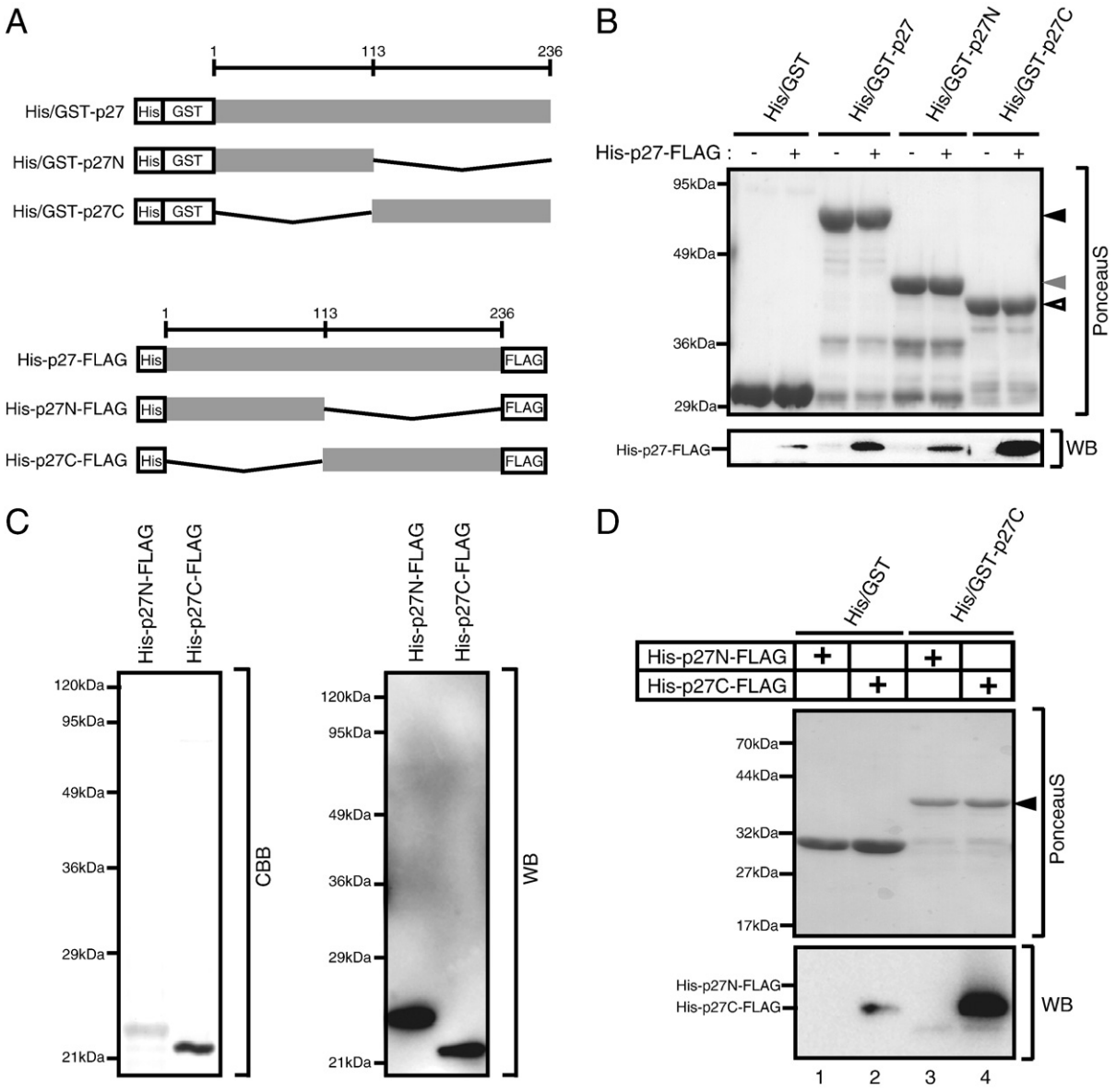

Fig. 2. The C-terminal half of p27 is responsible for p27–p27 interaction. (A) Schematic representation of His/GST-p27, His-p27-FLAG and their deletion mutants. Positions of amino acids are shown over His/GST-p27 and His-p27-FLAG. The boxes labeled His, GST and FLAG indicate the His-tag, the GST-tag and the FLAG-tag, respectively. Bent lines indicate the deleted amino acids. (B) *In vitro* interaction between His/GST-p27C and His-p27-FLAG. Glutathione resin-bound His/GST-p27, His/GST-p27N or His/GST-p27C was incubated with the purified His-p27-FLAG. Black, gray and white arrowheads, respectively, indicate His/GST-p27, His/GST-p27N and His/GST-p27C. For others, refer to the legend of Fig. 1B. (C) SDS-PAGE analysis of the purified His-p27N-FLAG and His-p27C-FLAG expressed in *E. coli*. The purified proteins (500 ng) were visualized with CBB staining (CBB), and analyzed by western blotting using anti-FLAG antibody (WB). (D) *In vitro* interaction between His/GST-p27C and His-p27C-FLAG. Glutathione resin-bound His/GST-p27C was incubated with the purified His-p27N-FLAG or His-p27C-FLAG. Black arrowhead indicates His/GST-p27C. For others, refer to the legend of Fig. 1B.

was not recovered by His/GST-p27C or by His/GST (Fig. 2D, lanes 1 and 3). In contrast, His-p27C-FLAG was recovered efficiently by His/GST-p27C (Fig. 2D, compare lane 2 with lane 4). These results indicate that the C-terminal half of p27 is responsible for p27–p27 interaction.

Next, to investigate which regions of p27 and p88 might be responsible for the p27–p88 interaction, we tested interactions of His/GST-p88 or His/GST-p88Δp27 with His-p27-FLAG, His-p27N-FLAG or His-p27C-FLAG by *in vitro* GST pull-down assays. His/GST-p88Δp27 lacks the region overlapping with p27 in p88 (Fig. 3A). His-p27-FLAG was recovered efficiently not only by His/GST-p88 but also by His/GST-p88Δp27 (Fig. 3B, lanes 4 and 7), indicating that the overlapping region in p88 is not essential for p27–p88 interaction. Furthermore, both His/GST-p88 and His/GST-p88Δp27 pulled down His-p27C-FLAG, but not His-p27N-FLAG (Fig. 3B, lanes 5, 6, 8 and 9), indicating that the C-terminal half of p27 is responsible for p27–p88 interaction. Together, these results suggest that p27–p88 interaction occurs through an interaction between the C-terminal half of p27 and the unique region of p88. However, it should be noted that these experiments cannot exclude the possibility that the overlapping region of p88 with p27 contributes to p27–p88 interaction.

To further delimit the regions in p27 responsible for p27–p27 and p27–p88 interactions, we constructed a series of deletion mutants using His-p27C-FLAG (Figs. 4A and B) and tested them for interactions with His/GST-p27C and His/GST-p88Δp27. *In vitro* GST pull-down assays revealed that deletion of 10 amino acids from the N-terminus of p27C did not interfere with the interactions with either His/GST-p27C or His/GST-p88Δp27 (Figs. 4C and D, lane 7). However, deletion of 30 amino acids from the N-terminus abolished or greatly reduced the ability of p27C to interact with His/GST-p27C and His/GST-p88p27, respectively (Figs. 4C and D, lane 8). Furthermore, deletions

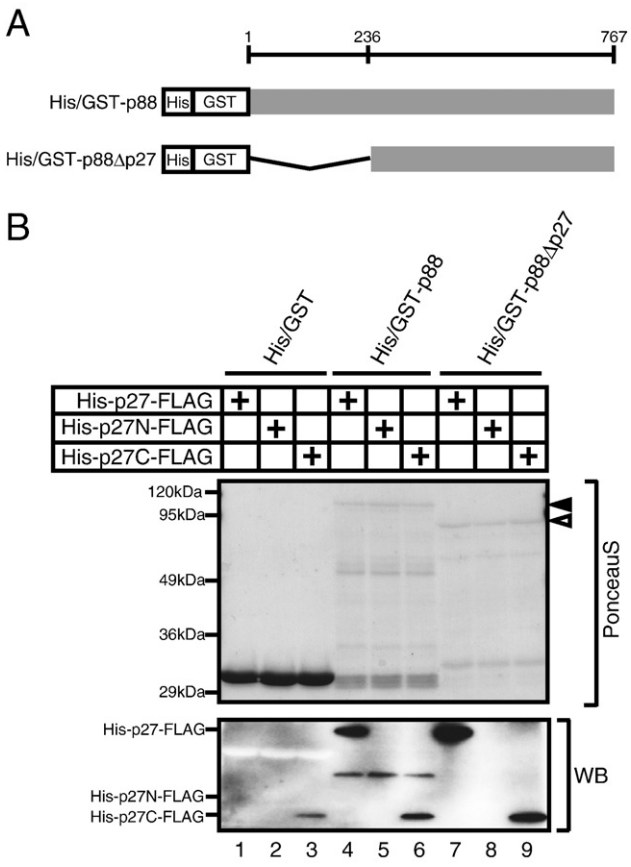

Fig. 3. The C-terminal half of p27 and the unique region of p88 are responsible for p27–p88 interaction. (A) Schematic representation of His/GST-p88 and His/GST-p88Δp27. His/GST-p88Δp27 lacks the region overlapping with p27 in p88. Positions of amino acids are shown over His/GST-p88. For others, refer to the legend of Fig. 2A. (B) Glutathione resin-bound His/GST-p88 or His/GST-p88Δp27 was respectively incubated with His-p27-FLAG, His-p27N-FLAG or His-p27C-FLAG. Black and white arrowheads, respectively, indicate His/GST-p88 and His/GST-p88Δp27. For others, refer to the legend of Fig. 1B.

of 10 and 30 amino acids from the C-terminus of p27C also caused deleterious effects on interactions with His/GST-p27C and His/GST-p88Δp27 (Figs. 4C and D, lanes 9 and 10). These results suggest that amino acid sequences from 124 to 236 in p27 are sufficient for p27–p27 and p27–p88 interactions.

Critical amino acid residues in the C-terminal half of p27 responsible for p27–p27 and p27–p88 interactions

To identify the critical amino acid residues of p27 involved in p27–p27 and p27–p88 interactions, we introduced mutations into the C-terminus region of p27 containing 30 amino acids. This was because the above results (Fig. 4) strongly implied the involvement of this region in p27–p27 and p27–p88 interactions and because the region contains tyrosine, phenylalanine and arginine residues conserved among dianthoviruses (Fig. 5), which could be involved in protein–protein interactions (Ma et al., 2003). The introduced mutations included single amino acid substitutions: such as tyrosine to alanine (Y_{207}A) or phenylalanine (Y_{207}F); arginine to alanine (R_{222}A) or lysine (R_{222}K); phenylalanine to alanine (F_{230}A) or tyrosine (F_{230}Y) and double amino acid substitutions, such as arginine to alanine ($RR_{214–215}$AA) or lysine ($RR_{214–215}$KK). To test the effects of the introduced mutations on p27–p27 and p27–p88 interactions, we used a cell-free *in vitro* assay system prepared from evacuolated BY-2 tobacco protoplasts (BYL) for coimmunoprecipitation experiments. This system has been used successfully to analyze the translation and replication mechanisms of RCNMV (Mizumoto et al., 2006; Iwakawa et al., 2007, 2008).

The effects of the mutations on p27–p27 interaction were examined by coimmunoprecipitation of C-terminally FLAG-tagged p27 (p27-FLAG) mutants with C-terminally HA-tagged wild-type p27 (p27-HA). Substitutions of Y_{207}, $RR_{214–215}$ or R_{222} to alanine strongly inhibited coimmunoprecipitation of the mutant p27s with p27-HA (Fig. 6A, lanes 2, 4 and 6). A similar deleterious effect was observed when two arginine residues ($RR_{214–215}$) were substituted with a similar positively charged lysine (Fig. 6A, lane 5), whereas only a moderate inhibitory effect was observed when R_{222} was substituted with lysine (Fig. 6A lane 7). However, substitution of Y_{207} with the similar aromatic amino acid, phenylalanine caused mild or no deleterious effects on coimmunoprecipitation with p27-HA (Fig. 6A, lane 3, data not shown). No or mild deleterious effects were also observed when F_{230} was substituted with alanine or a similar aromatic amino acid, tyrosine (Fig. 6A, lanes 8 and 9, data not shown). These results suggest that an aromatic residue at position 207 (Y_{207}) and arginines at positions 214 and 215 ($RR_{214–215}$) are important for p27–p27 interaction, and that arginine at position 222 (R_{222}) has an important role for p27–p27 interaction although this arginine could be replaced with lysine.

Next, we investigated the effects of the mutations on p27–p88 interaction as described above by coimmunoprecipitation of p27-FLAG mutants with C-terminally T7-tagged wild-type p88 (p88-T7) in the presence of RNA2. When Y_{207}, $RR_{214–215}$, or R_{222} were substituted with alanine, coimmunoprecipitation of these mutant p27s with p88-T7 was inhibited strongly (Fig. 6B, lanes 2, 4 and 6). Interestingly, substitution of F_{230} with alanine, which did not disturb the interaction with p27-HA, inhibited the coimmunoprecipitation with p88-T7 (Fig. 6B, lane 8). A similar inhibitory effect was observed when two arginines ($RR_{214–215}$) were substituted with similar positively charged lysines (Fig. 6B, lane 5). However, substitutions of Y_{207} or F_{230} with a similar aromatic phenylalanine (Y_{207}F) or tyrosine (F_{230}Y), respectively, did not affect coimmunoprecipitation with p88-T7 (Fig. 6B, lanes 3 and 9). Substitution of arginine at the R_{222} position with a similar positive-charged lysine, which moderately inhibited interaction with p27-HA, also had no effect on coimmunoprecipitation with p88-T7 (Figs. 6A and B, lane 7). These results suggest that aromatic residues at the Y_{207} and F_{230} positions as well as arginines at the $RR_{214–215}$ positions appear to be important for p27–p88 interactions, and that a positively charged amino acid at R_{222} seems to have an important role in p27–p88 interaction.

Effects of point mutations that affect p27–p27 and p27–p88 interactions on the formation of 380-kDa and 480-kDa complexes

We demonstrated previously that RCNMV replicase proteins form the 380-kDa and the 480-kDa complexes (Mine et al., 2010). The 380-kDa complex contains p27 as a virus-derived component, whereas the 480-kDa complex contains both p27 and p88. Importantly, the 480-kDa complex exhibits template-dependent RdRP activity by recognizing the 3′ terminal core promoter sequences of RCNMV genomic RNAs 1 and 2, suggesting its central role in viral RNA synthesis. To test the effects of the point mutations in p27 that affected p27–p27 and p27–p88 interactions on the assembly of these complexes, we analyzed the accumulated levels of the 380-kDa and the 480-kDa complexes using blue-native polyacrylamide gel electrophoresis (BN-PAGE) in BYL. When p27-FLAG with mutations that compromised p27–p27 interaction were singly expressed in BYL, the 380-kDa complex was not detected (Fig. 7A, lanes 3, 5, 6, 7 and 8), whereas the 380-kDa complexes accumulated in BYL in incubation with p27-FLAG mutants retaining the ability to interact with each other (Fig. 7A, lanes 4, 9 and 10). These results suggest that p27–p27 interaction is required for the formation of the 380-kDa complex.

When p27-FLAG mutants were expressed together with p88-T7 and RNA2, the 480-kDa complex accumulated in BYL incubated with p27-FLAG Y_{207}F, p27-FLAG R_{222}K and p27-FLAG F_{230}Y, which still have

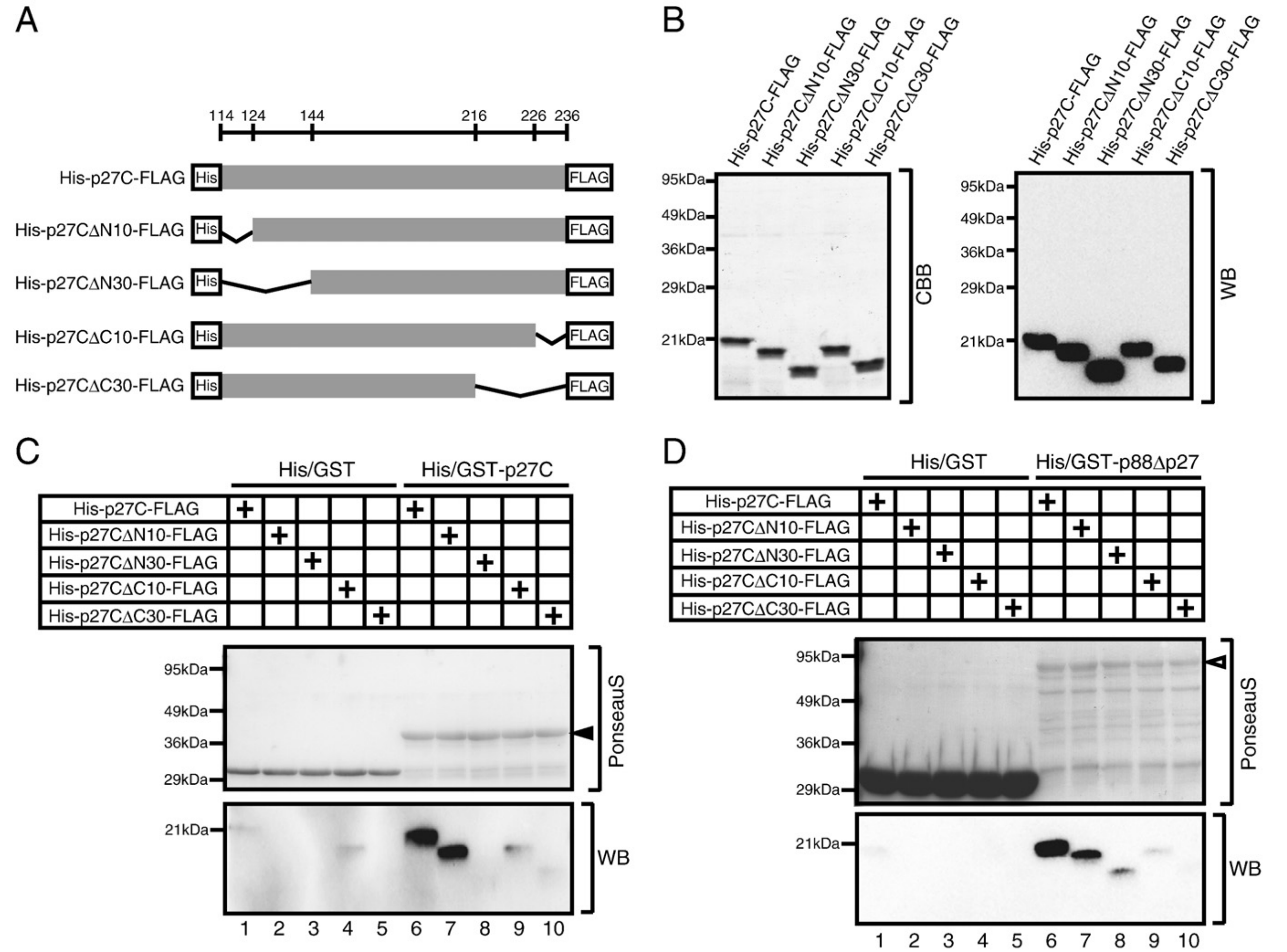

Fig. 4. Determination of the region within p27 that is responsible for p27–p27 and p27–p88 interactions. (A) Schematic representation of His-p27C-FLAG deletion mutants. Positions of amino acids are shown over His-p27C-FLAG. For others, refer to the legend of Fig. 2A. (B) SDS-PAGE analysis of purified His-p27C-FLAG deletion derivatives expressed in *E. coli*. For others, refer to the legend of Fig. 2C. (C and D) *In vitro* interactions of His-p27C-FLAG or its derivatives with His/GST-p27C and His/GST-p88Δp27. His-p27C-FLAG or its mutants were incubated with glutathione resin-bound His/GST-p27C (C) or His/GSTp88Δp27 (D). Black and white arrowheads, respectively, indicate His/GST-p27C and His/GST-p88p27. For others, refer to the legend of Fig. 1B.

the ability to interact with both p27 and p88, although the accumulated levels of the complex differed among these p27-FLAG mutants (Fig. 7B, lanes 4, 8 and 10). On the other hand, the 480-kDa complex was undetectable after incubation with the rest of the mutants including p27-FLAG F_{230}A (Fig. 7B, lanes 3, 5, 6, 7 and 9), which has a mutation compromising only p27–p88 interaction (Fig. 6). These results suggest that p27–p27 interaction is not sufficient, and p27–p88 interaction is required for the formation of the 480-kDa complex.

Roles of p27–p27 and p27–p88 interactions in negative-strand RNA synthesis in vitro

To investigate the roles of p27–p27 and p27–p88 interactions in negative-strand RNA synthesis, we tested p27-FLAG mutants for their ability to accumulate negative-strand RNAs in BYL in the presence of p88-T7 and RNA2. Note that negative-strand RNA can be synthesized from an RNA1 mutant expressing p88-T7 in a *cis*-preferential manner because this RNA1 mutant merely lacks an almost entire CP-coding region that is not essential for RNA1 replication (Okamoto et al., 2008). Northern blot analysis showed that p27-FLAG mutants with mutations that compromised both p27–p27 and p27–p88 interactions (Fig. 6) abolished or greatly reduced the accumulated levels of negative-strand RNAs of both RNA1 and RNA2 (Fig. 8, lanes 3, 5–7). Those p27-FLAG mutants with mutations that compromised either p27–p27 or p27–p88 interaction supported negative-strand RNA accumulations with reduced levels compared with wild-type p27 (Fig. 8, lanes 4, 8, 9 and 10). Interestingly, the accumulated levels of negative-strand RNAs corresponded to those of the 480-kDa complex (Figs. 7B and 8). Western blot analysis showed that the accumulated

```
        114       124                 144             206                    236
                                                       *     **   *    *
RCNMV  MKLQRSAARKHIKRVRPGMMQAAIKAVETRIRNRH[...]DSVKLAYNPKSQARRTLVSAIRENAVAGFKSLEDF
SCNMV  MVLQRSAARKHIKRVRAGMMQAAIKAVEKRIRNRH[...]DSVKLAYNPKSQARRTLVTAVRENAVAGFKSLEDF
CRSV   MKLKRVAARRQIKRVRSGMIEDAISAVEARIRNRH[...]DATKMAYNPKSQARRDLVSILRKNISFGFKSLEDF
```

Fig. 5. Sequence alignments of the region within p27 involved in p27–p27 and p27–p88 interactions in RCNMV and other dianthoviruses. Amino acids contained in the region, which is involved in p27–p27 and p27–p88 interactions, are shown with bold-faced letters. Asterisks indicate the conserved amino acids selected for mutagenesis in RCNMV p27. The following abbreviations were used: SCNMV, *Sweet clover necrotic mosaic virus*; CRSV, *Carnation ring spot virus*.

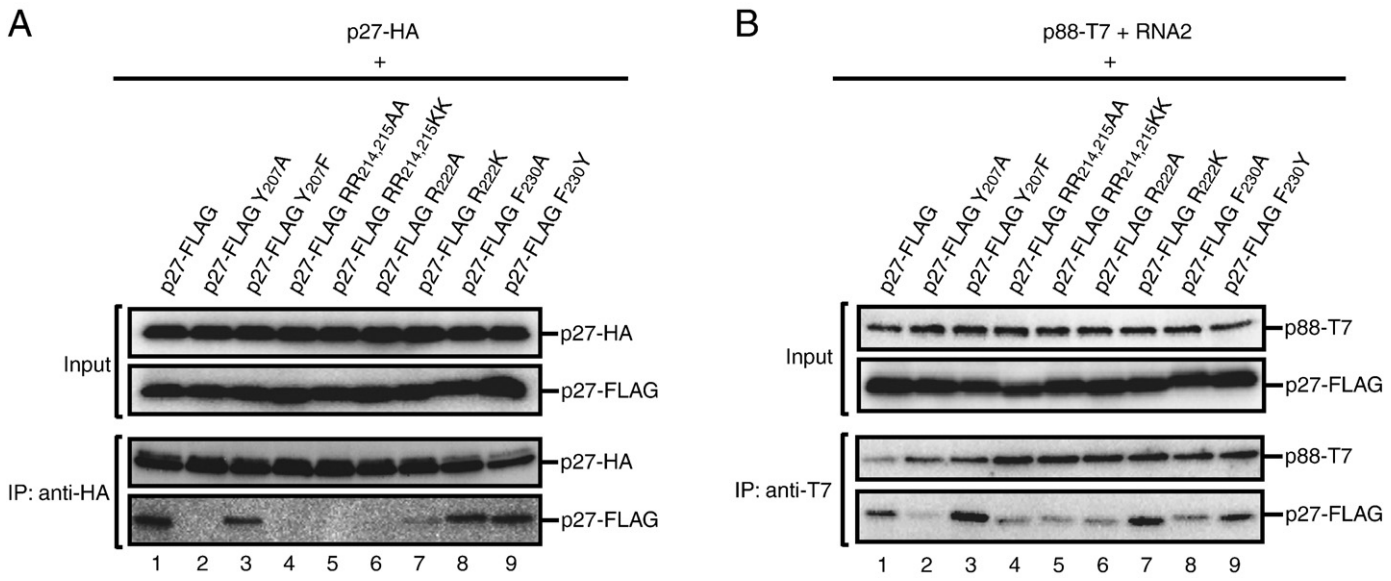

Fig. 6. Effects of mutations introduced into p27 on interactions between RCNMV replicase proteins. (A) Coimmunoprecipitation analysis of the interactions between p27-HA and p27-FLAG mutants. Transcripts that express p27-HA and p27-FLAG mutants were incubated in BYL. After 4 h of incubation, the membrane fractions of BYL were solubilized and subjected to immunoprecipitation with anti-HA antibody, followed by western blotting using anti-HA antibody and anti-FLAG antibody. (B) Coimmunoprecipitation analysis of the interactions between p88-T7 and p27-FLAG mutants. Transcripts that express p88-T7 and p27-FLAG mutants were incubated together with RNA2 in BYL. After 4 h of incubation, the membrane fractions of BYL were solubilized and subjected to immunoprecipitation with anti-T7 antibody, followed by western blotting using anti-T7 antibody and anti-FLAG antibody.

levels of p27-FLAG and p88-T7 were similar in all incubations (data not shown). These results suggest that both p27–p27 and p27–p88 interactions play important roles in negative-strand RNA synthesis via assembly of the 480-kDa complex.

Viral RNA replication and suppression of RNA silencing in vivo

Our previous study demonstrated that RCNMV suppresses RNA silencing by using three viral components, p27, p88 and viral RNAs, which support at least negative-strand RNA synthesis (Takeda et al., 2005). This suggests a strong link between RCNMV RNA replication and the suppression of RNA silencing. To test whether the 480-kDa complex formation might be associated with the suppression of RNA silencing by RCNMV, we co-expressed p27-FLAG mutants, p88-T7 and RNA2 with green fluorescent protein (GFP) mRNA as an inducer of RNA silencing, using an *Agrobacterium*-mediated expression system in GFP-expressing *N. benthamiana* line 16c (Takeda et al., 2005). We analyzed the accumulations of GFP mRNA, GFP-specific small interfering RNAs (siRNAs), and viral RNAs by northern blotting, and the accumulations of viral proteins and their complexes by western blotting at 4 days post infiltration (dpi). Consistent with the *in vitro* results, the accumulated levels of positive- and negative-strand RNA2 correlated well with those of the 480-kDa complex but not with the 380-kDa complex (Figs. 9A and B), suggesting that the former functions as RCNMV replicase complex *in vivo* as well as *in vitro* (Mine et al., 2010). Furthermore, the accumulated levels of GFP mRNA corresponded to those of the 480-kDa complex (Figs. 9A and B), and the accumulated levels of GFP-specific siRNAs were inversely correlated with those of GFP mRNA (Fig. 9A). These results suggest that suppression of RNA silencing activity of RCNMV depends on the accumulated levels of the 480-kDa but not of the 380-kDa complex. The accumulated levels of p27-FLAGs also corresponded to that of the 480-kDa complex (Figs. 9A and B), although all p27-FLAG proteins tested accumulated at comparable levels in *Agrobacterium*-infiltrated leaves at 2 dpi (data not shown). These results suggest that RCNMV RNA replication, including the formation of the 480-kDa complex, is important for a sustainable accumulation of viral replicase proteins. Overall, the good correlation between suppression of RNA silencing activity and the accumulated levels of the 480-kDa complex suggests that the formation of the 480-kDa complex plays an important role in suppression of RNA silencing.

Discussion

Our previous study demonstrated that the 480-kDa complex containing p27, p88 and possible host proteins has RCNMV-specific and template-dependent RdRP activity (Mine et al., 2010), suggesting a central role of this complex in RCNMV RNA replication. Here we found that only p27 and its mutants that have the ability to interact with both p27 and p88 are capable of forming the 480-kDa complex. These p27 proteins together with p88 and viral RNAs supported viral RNA replication, and the accumulated levels of viral RNAs corresponded to that of the 480-kDa complex, suggesting that the 480-kDa complex functions as an RCNMV replicase complex. We also found that suppression of RNA silencing activity of RCNMV corresponded to the accumulated levels of the 480-kDa complex. Overall, our studies indicate that interactions between p27 and p88 replicase proteins play an essential role in viral RNA replication and suppression of RNA silencing via the assembly of the 480-kDa RCNMV replicase complex.

GST pull-down experiments using purified recombinant p27 and p88 demonstrated that p27 can interact with both p27 and p88 through direct protein–protein contacts (Fig. 1B), and that the C-terminal half of p27 is responsible for both p27–p27 and p27–p88 interactions (Figs. 2 and 3). Interestingly, although p88 possesses a region overlapping with p27 in its N-terminal portion, this is not essential for p27–p88 interaction (Fig. 3). These results suggest that interaction between p27 and p88 occurs through protein–protein contacts between the C-terminal half of p27 and the unique region of p88. The functional significance of this is supported by our finding that the unique region of p88 alone together with p27 was able to support negative-strand RNA2 synthesis in BYL, albeit at a lower level than wild-type p88 (Supplementary Fig. 1).

In contrast to RCNMV p27 and p88, the N-terminally overlapping p33 and p92 replicase proteins of TBSV interact with each other through interaction domains located in the overlapping region, and

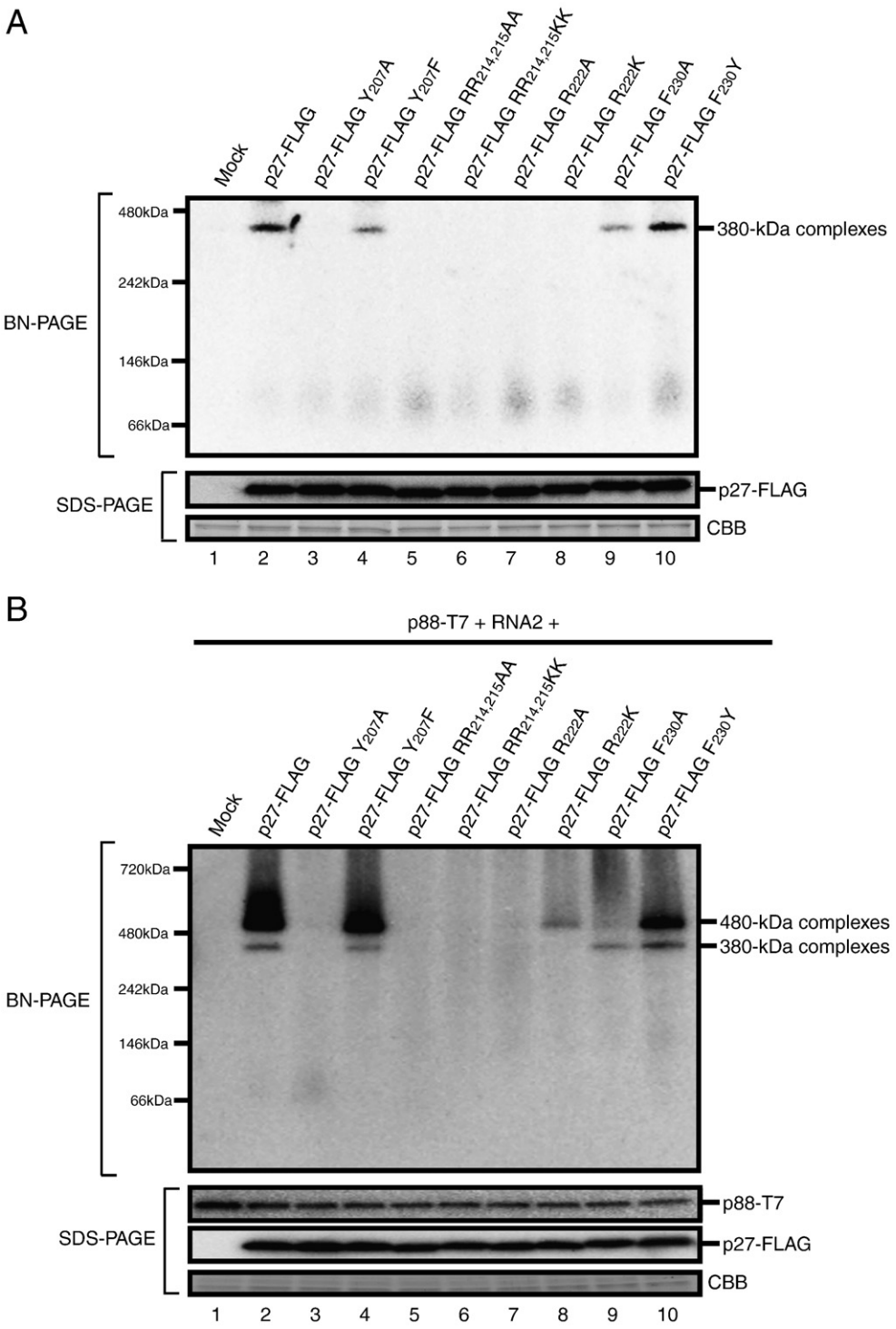

Fig. 7. Effects of mutations introduced into p27 on the formation of the 380-kDa and the 480-kDa complexes. Accumulations of the 380-kDa complex in BYL incubated with transcripts that express p27-FLAG mutants (A), and accumulations of the 480-kDa complex in BYL incubated with transcripts that express p27-FLAG mutants and p88-T7 in the presence of RNA2 (B). After 4 h of incubation, the solubilized membrane fractions were subjected to BN-PAGE (upper panel) and SDS-PAGE (lower panel), followed by western blotting with appropriate antibodies.

the unique region of p92 polymerase does not participate in this interaction (Rajendran and Nagy, 2004). A similar arrangement of interaction domains is reported for TMV 126K and 183K replicase proteins, which possess N-terminally overlapping methyltransferase and helicase-like domains. The C-terminal helicase-like domain of the 126K protein interacts with the corresponding region in 183K, while the unique region of the 183K protein carrying the RdRP motif is not involved in this interaction (Goregaoker et al., 2001). Thus, RCNMV seems to employ an interaction mechanism to form the viral replicase complex that differs from other viruses such as TBSV and TMV, which have N-terminally overlapping replicase proteins.

We identified critical amino acid residues within p27 required for p27–p27 and p27–p88 interactions by mutational analysis (Fig. 6). Furthermore, BN-PAGE analysis demonstrated that p27 with mutations that compromise the p27–p27 interaction failed to form the 380-kDa complex, whereas p27 with mutations that did not compromise the p27–p27 interaction did so (Fig. 7A). These results supported our previous report that the 380-kDa complex could be an

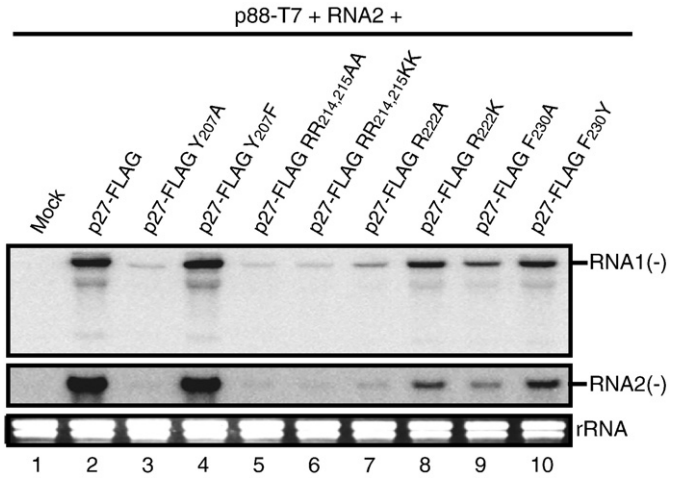

Fig. 8. Effects of mutations introduced into p27 on negative-strand RNA synthesis. Transcripts that express p27-FLAG mutants and p88-T7 were incubated together with RNA2 in BYL. After 4 h of incubation, accumulations of negative-strand RNAs in total RNA extracts were analyzed by northern blotting.

oligomeric form of p27. In addition, we found that only p27-FLAG $Y_{207}F$, p27-FLAG $R_{222}K$ and p27-FLAG $F_{230}Y$, among the p27 mutants tested that are functional for both p27–p27 and p27–p88 interactions led to the formation of the 480-kDa complex, suggesting important roles of p27–p27 and p27–p88 interactions in the assembly of the 480-kDa complex.

Of the p27 mutants, p27-FLAG $R_{222}K$ and p27-FLAG $F_{230}Y$ deserve further discussion. p27-FLAG $R_{222}K$ failed to form the 380-kDa complex (p27-oligomer) at detectable levels, probably because the $R_{222}K$ mutation inhibited p27–p27 interaction (Figs. 6A and 7A). However, this mutation did not inhibit p27–p88 interaction (Fig. 6B, data not shown), but significantly inhibited the formation of the 480-kDa complex (Fig. 7B). These results suggest that p27 oligomerization is a critical step. On the other hand, the $F_{230}A$ mutation that compromised p27–p88 interaction but had little effect on the p27–p27 interaction (Fig. 6) did not inhibit p27 oligomerization (Fig. 7A), but almost completely disrupted the formation of the 480-kDa complex (Fig. 7B). This suggests that p27 oligomerization is insufficient and that p27–p88 interaction is required for the assembly of the 480-kDa complex. Based on these findings, it appears that the formation of the 480-kDa complex is directed through the p27-oligomer (the 380-kDa complex) interacting with p88 protein(s).

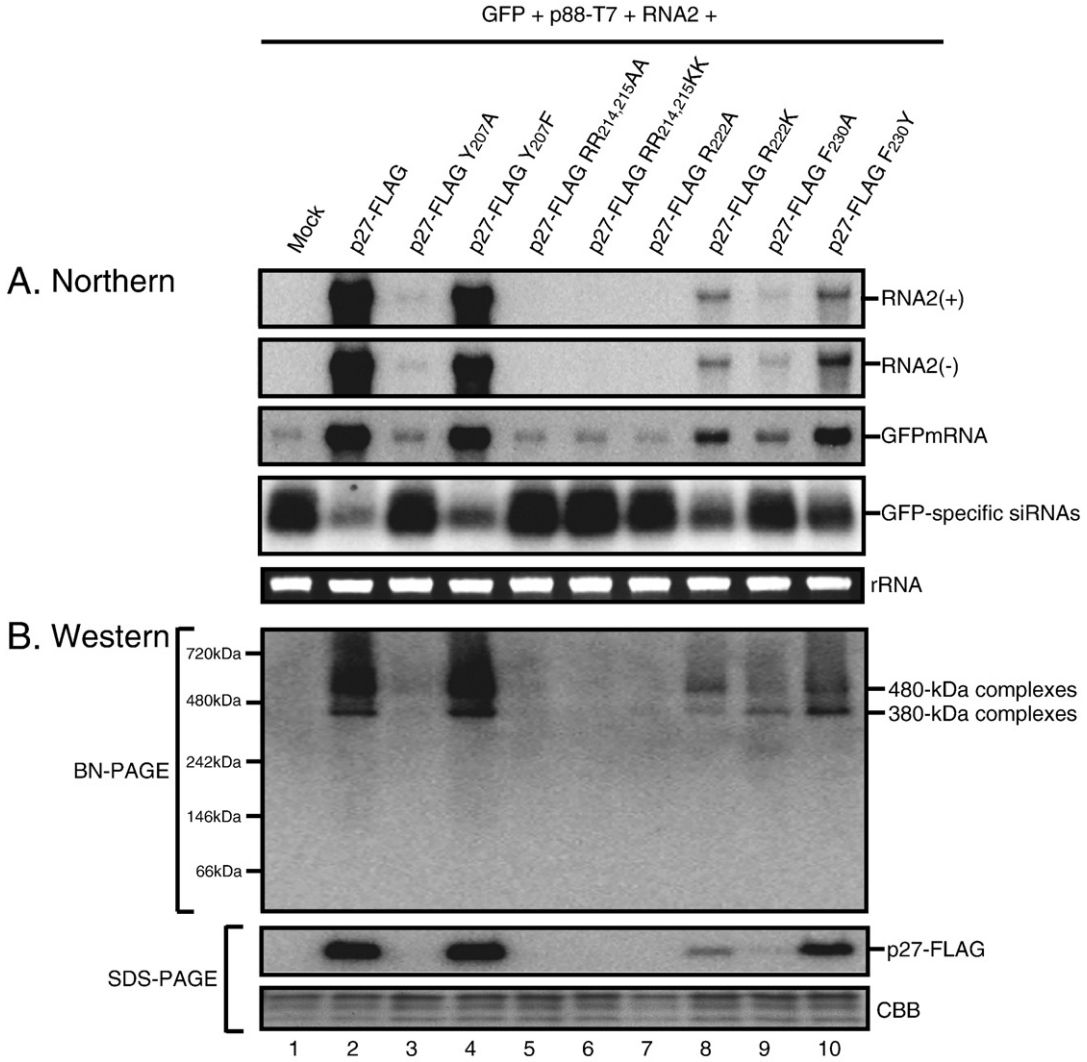

Fig. 9. Effects of mutations introduced into p27 on viral RNA replication and suppression of RNA silencing. p27-FLAG or its mutants were expressed together with p88-T7, RNA2 and GFP mRNA in leaves of GFP-expressing *N. benthamiana* (line 16c) by *Agrobacterium*-infiltration. (A) Northern blot analysis of viral RNAs, GFP mRNA and GFP-specific siRNAs. Total RNAs were extracted at 4 days after infiltration. (B) Western blot analysis of p27-FLAG mutants and their complexes. Protein samples were extracted from the membrane fractions of *Agrobacterium*-infiltrated leaves and subjected to BN-PAGE and SDS-PAGE, followed by western blotting with anti-FLAG antibody.

What is the functional significance of the 480-kDa complex assembly? Viral replicase proteins of several plant- and animal-infecting viruses form highly ordered complexes to enhance their functionality. For instance, electron microscopy of purified polypeptides containing helicase domains within the overlapping regions of 126K and 183K TMV replicase proteins suggested that TMV replicase proteins form hexameric ring-like structures (Goregaoker and Culver, 2003). This hexameric structure is likely to be important for the helicase activity of TMV replicase protein because several DNA and RNA helicases function as hexamers (Kadare and Haenni, 1997; Patel and Picha, 2000). However, the formation of the 480-kDa complex is unlikely to be related to the helicase activity of RCNMV replicase proteins that lack an RNA helicase domain (Koonin and Dolja, 1993), although it is possible that host proteins recruited to the complex function as helicases.

The formation of the 480-kDa complex might have other functions such as enhancing RNA binding ability. It is known that oligomerization of poliovirus 3D polymerase through two protein–protein interfaces is important for its RNA binding activity (Hobson et al., 2001). Human immunodeficiency virus Rev protein, which is known to recognize the Rev response element (RRE), has been shown to form oligomers and thereby promote binding to RRE (Daugherty et al., 2008). Furthermore, the interaction domain of TBSV p33 replicase protein is required for specific recognition of template RNAs *in vitro* (Pogany et al., 2005). Thus, it is possible that the formation of the 480-kDa complex enhances RNA binding activity and/or specificity of template RNA recognition, and thereby promotes viral RNA replication. Alternatively, the formation of the 480-kDa complex could be important for the catalytic activity of p88. In fact, oligomerization of hepatitis C virus NS5B is critical for its RdRP activity (Qin et al., 2002; Wang et al., 2002). Determining the crystal structure of the 480-kDa complex might explain the functional significance of such a highly ordered complex formation by RCNMV replicase proteins.

Takeda et al. (2005) showed a strong link between the suppression of RNA silencing by RCNMV and viral RNA replication: the expression of p27 or p88 or both failed to suppress RNA silencing in the absence of negative-strand synthesis- or replication-competent RNAs. This suggests that formation of the RCNMV replicase complex and/or viral RNAs synthesized by the replicase complex are required for suppressing RNA silencing. Consistent with this, our study showed a strong correlation between the suppression of RNA silencing activity and the accumulated levels of the 480-kDa complex, which also correlates with viral RNA replication levels (Figs. 9A and B). Recently, we have identified several host proteins as candidates for the components of the 480-kDa complex (Mine et al., 2010). It is possible that recruitment of these to the 480-kDa complex contributes to the suppression of RNA silencing by RCNMV. However, at present, we do not know what carries out the suppression of RNA silencing. Further studies are needed to dissect the mechanism of suppression of RNA silencing by RCNMV.

In summary, we propose a model for the formation of the RCNMV replicase complex (Fig. 10). In RCNMV-infected cells, p27 forms a 380-kDa oligomer following efficient translation from RNA1, which could occur before the translation of p88 produced by ribosomal frameshifting at much lower frequency (Kim and Lommel, 1994). After p88 is translated by ribosomal frameshifting, the 480-kDa complex is formed via interaction of p88 with p27-oligomers and possibly via interaction with host proteins (Mine et al., 2010). Then, this 480-kDa replicase complex initiates viral RNA replication via complementary RNA synthesis at the endoplasmic reticulum membrane (Turner et al., 2004; Mine et al., 2010), and contributes to suppression of RNA silencing by an as-yet-unidentified mechanism. At present, this model is likely incomplete because of limited information on other functions of p27 and p88, viral RNA elements and host proteins that could also be involved in the formation of RCNMV replicase complex (Mine et al., 2010).

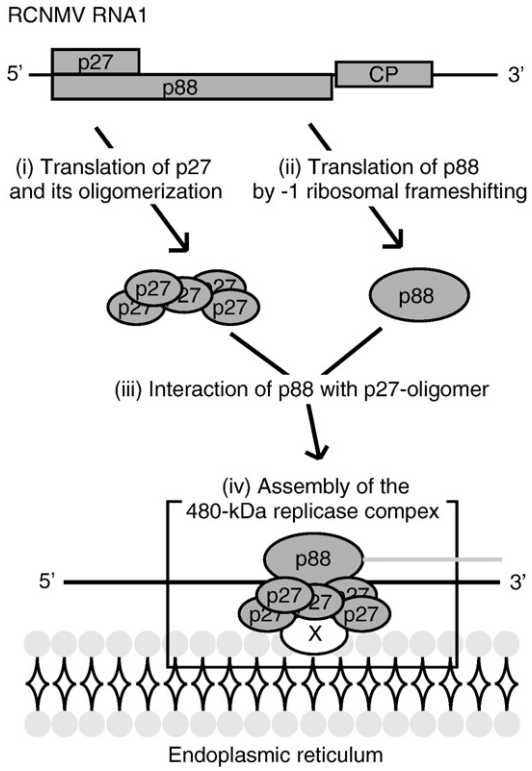

Fig. 10. A model for the roles of p27–p27 and p27–p88 interactions in the formation of RCNMV replicase complexes. (i) p27 is translated efficiently from RNA1, and forms the 380-kDa oligomer. (ii) p88 is translated from RNA1 via programmed −1 ribosomal frameshifting at much lower frequency (Kim and Lommel, 1994). (iii and iv) the 480-kDa complex is formed via interaction of p88 with p27-oligomers and possibly via interaction with host proteins (Mine et al., 2010). Then, this 480-kDa replicase complex initiates viral RNA synthesis on the endoplasmic reticulum membrane, and contributes to suppression of RNA silencing by an as-yet-unidentified mechanism.

Materials and methods

Plasmid construction

pUCR1 (Takeda et al., 2005) and pRC2|G (Xiong and Lommel, 1991) are full-length cDNA clones of RNA1 and RNA2 of RCNMV Australian strain, respectively. Constructs described previously that were used in this study include pBICp27-iFLAG (Mine et al., 2010), pBICp27-HA (Mine et al., 2010), pBICp88-T7 (Mine et al., 2010), pBICGFP (Takeda et al., 2005) and pBICRC2 (Takeda et al., 2005). pUC118 and pCold I vectors were purchased from TAKARA Bio Inc. (Shiga, Japan). All plasmids constructed in this study were verified by sequencing. The sequences of the primers used in this study are listed in Table 1.

pColdp27-FLAG, pColdp27N-FLAG and pColdp27C-FLAG

DNA fragments were amplified by polymerase chain reaction (PCR) from pBICp27-FLAG. The primer pairs used for the construction of pColdp27-FLAG, pColdp27N-FLAG, and pColdp27C-FLAG were *Kpn*I-p27-F plus *Kpn*I-p27-FLAG-R, *Kpn*I-p27-F plus *Kpn*I-p27N-FLAG-R, and *Kpn*I-p27C-F plus *Kpn*I-p27-FLAG-R, respectively. The amplified DNA fragments were digested with *Kpn*I, and cloned into *Kpn*I-digested pCold I.

pColdp27CΔN10-FLAG, pColdp27CΔN30-FLAG, pColdp27CΔC10-FLAG and, pColdp27CΔC30-FLAG

DNA fragments were amplified by PCR from pColdp27C-FLAG. The primer pairs used for the construction of pColdp27CΔN10-FLAG and pColdp27CΔN30-FLAG were *Kpn*I-p27-FLAG-R plus *Kpn*I-p27CΔN10-F

Table 1
List of primers and their sequences used for PCR to generate constructs.

Primer	Sequence
*Kpn*I-p27-F	CGGGGTACCATGGGTTTTATAAATCTTTC
*Kpn*I-p27-FLAG-R	CGGGGTACCCTACTTGTCATCGTCGTCC
*Kpn*I-p27N-FLAG-R	CGGGGTACCCTACTTGTCATCGTCGTCCTTGTAATCCACGCCTTCCTCATCCTTC
*Kpn*I-p27C-F	CGGGGTACCATGAAACTCCAAAGGAGCGCTGC
*Kpn*I-p27CΔN10-F	GCTCGGTACCATTAAACGTGTGCPrGCCCAGG
*Kpn*I-p27CΔN30-F	GCTCGGTACCAGAAATCGCCATACCATCTT
*Kpn*I-p27CΔC10-FLAG-R	GCTCGGTACCCTACTTGTCATCGTCGTCCTTGTAATCAGCCTTGTTCTCACGAATGG
*Kpn*I-p27CΔC30-FLAG-R	GCTCGGTACCCTACTTGTCATCGTCGTCCTTGTAATCGGCGAGCTTGACGCTGTCGA
*Nde*I-GST-F	CCGGAATTCATATGTCCCCTATACTAGGTTATTGG
*Nde*I-3C-GST-R	CCGGAATTCATATGGGGCCCCTGGAACAGAACTTCCAGATCCGATTTTGGAGGATGGTC
*Kpn*I-p27-R	CGGGGTACCCTAAAAATCCTCAAGGGATT
*Kpn*I-p27N-R	CGGGGTACCCTACACGCCTTCCTCATCCTT
*Kpn*I-p88-R	CGGGGTACCTTATCGGGCTTTGATTAGATC
*Kpn*I- p88Δp27-F	CGGGGTACCTTAGGCGGCCCACTCAGCTTT
*Mlu*I-FLAG-R	TTGCACGCGTCTACTTGTCATCGTCGTCCTTGTAATCAAAATCCTCAAGGG
*Mlu*I-HA-R	TTGCACGCGTCTAAGCGTAATCTGGAACATCGTATGGGTAAAAATCCTCAAGGG
*Mlu*I-T7-R	TTGCACGCGTTTATCCCATTTGTTGACCACCTGTCATAGAAGCCATTCGGGCTTTGATTAGATC
pUC*Sac*I-F	AATTTCACACAGGAAACAGC
p27-22R	AGCAGATGGAACGTGTAG
BIC*Dra*III-F	AAGGGCGAAAAACCGTCTA
BIC*Hind*III-R	AAACAGCTATGACCATGATT
$p27Y_{207}A$-F	TCTTAGGATTGGCGGCGAGCTTG
$p27Y_{207}A$-R	CAAGCTCGCCGCCAATCCTAAGA
$p27Y_{207}F$-F	TCTTAGGATTGAAGGCGAGCTTG
$p27Y_{207}F$-R	CAAGCTCGCCTTCAATCCTAAGA
$p27RR_{214-215}AA$-F	AAACCAAAGTGGCGGCGGCTTGACT
$p27RR_{214-215}AA$-R	GAGTCAAGCCGCCGCCACTTTGGTT
$p27RR_{214-215}KK$-F	AAACCAAAGTCTTCTTGGCTTGACT
$p27RR_{214-215}KK$-R	GAGTCAAGCCAAGAAGACTTTGGTT
$p27R_{222}A$-F	CCTTGTTCTCGGCAATGGCTGAA
$p27R_{222}A$-R	TTCAGCCATTGCCGAGAACAAGG
$p27R_{222}K$-F	CCTTGTTCTCCTTAATGGCTGAA
$p27R_{222}K$-R	TTCAGCCATTAAGGAGAACAAGG
$p27F_{230}A$-F	CAAGGGATTTGGCCCCGGCAACA
$p27F_{230}A$-R	TGTTGCCGGGGCCAAATCCCTTG
$p27F_{230}Y$-F	CAAGGGATTTGTACCCAGCAACA
$p27F_{230}Y$-R	TGTTGCTGGGTACAAATCCCTTG
nGFP-F	AACCGGTTAAGCTTATGAGTAAAGGAGAAGAACT
T7-nGFP-R	AACCGGTTGAATTCTAATACGACTCACTATAGTTATTTGTATAGTTCATCCA
p88Δp27-F	ACCAGTCATGTTAGGCGGCCCACTCAGCTT
p88Δp27-R	GGCCGCCTAACATGACTGGTACGAAAAGTA

and *Kpn*I-p27-FLAG-R plus *Kpn*I-p27CΔN30-F, respectively. The primer pairs used for the construction of pColdp27CΔC10-FLAG and pColdp27CΔC30-FLAG were *Kpn*I-p27C-F plus *Kpn*I-p27CΔC10-FLAG-R and *Kpn*I-p27C-F plus *Kpn*I-p27CΔC30-FLAG-R, respectively. The amplified DNA fragments were digested with *Kpn*I, and cloned into *Kpn*I-digested pCold I.

pColdGST

A PCR fragment was amplified by PCR from pGEX-2TK (GE Healthcare, Little Chalfont, Buckinghamshire, UK) using the primer pair, *Nde*I-GST-F plus *Nde*I-3C-GST-R. The amplified DNA was digested with *Nde*I, and cloned into *Nde*I-digested pCold I.

pColdGST-p27, pColdGST-p27N and pColdGST-p27C

DNA fragments were amplified by PCR from pColdp27-FLAG. The primer pairs used for the construction of pColdGST-p27, pColdGST-p27N, and pColdGST-p27C were *Kpn*I-p27-F plus *Kpn*I-p27-R, *Kpn*I-p27-F plus *Kpn*I-p27N-R, and *Kpn*I-p27C-F plus *Kpn*I-p27-R, respectively. The amplified DNA fragments were digested with *Kpn*I, and cloned into *Kpn*I-digested pColdGST.

pColdGST-p88 and pColdGST-p88Δp27

DNA fragments were amplified by PCR from pBICp88-T7. The primer pairs used for the construction of pColdGST-p88 and pColdGST-p88Δp27 were *Kpn*I-p27-F plus *Kpn*I-p88-R and *Kpn*I-p88Δp27-F plus *Kpn*I-p88-R, respectively. The amplified DNA fragments were digested with *Kpn*I, and cloned into *Kpn*I-digested pColdGST.

pUCp27-FLAG, pUCp27-HA, and pUCp88-T7

To construct pUCp27-FLAG, DNA fragments were amplified from pBICp27-iFLAG using the primer pair, p27-22R and *Mlu*I-FLAG-R. To construct pUCp27-HA, DNA fragments were amplified from pBICp27-HA using the primer pair, p27-22R and *Mlu*I-HA-R. To construct pUCp88-T7, DNA fragments were amplified from pBICp88-T7 using the primer pair p27-22R and *Mlu*I-T7-R. These amplified DNA fragments were digested with *Tth111*I and *Mlu*I, and used to replace the small *Tth111*I–*Mlu*I region of pUCR1.

pUCp27-FLAG $Y_{207}A$, pUCp27-FLAG $Y_{207}F$, pUCp27-FLAG $RR_{214-215}AA$, pUCp27-FLAG $RR_{214-215}KK$, pUCp27-FLAG $R_{222}A$, pUCp27-FLAG $R_{222}K$, pUCp27-FLAG $F_{230}A$, and pUCp27-FLAG $F_{230}Y$

DNA fragments were amplified from pUCp27-FLAG. The primer pairs used were pUC*Sac*I-F plus one each of the following: $p27Y_{207}A$-R, $p27Y_{207}F$-R, $p27RR_{214-215}AA$-R, $p27RR_{214-215}KK$-R, $p27R_{222}A$-R, $p27R_{222}K$-R, $p27F_{230}A$-R and $p27F_{230}Y$-R. Another primer *Mlu*I-FLAG-R was used together with one each of the following: $p27Y_{207}A$-F, $p27Y_{207}F$-F, $p27RR_{214-215}AA$-F, $p27RR_{214-215}KK$-F, $p27R_{222}A$-F, $p27R_{222}K$-F, $p27F_{230}A$-F and $p27F_{230}Y$-F. Each recombinant PCR product was amplified by using pUC*Sac*I-F and *Mlu*I-FLAG-R,

digested with *Sac*I and *Mlu*I, and inserted into the corresponding region of pUCp27-FLAG.

pUCp88Δp27-T7

Two DNA fragments were amplified from pUCp88-T7 using two sets of primers, pUC*Sac*I-F plus p88Δp27-R and p88Δp27-F plus *Mlu*I-T7-R. Then, DNA fragments were amplified from a mixture of these two PCR fragments by using the primer pair, pUC*Sac*I-F plus *Mlu*I-T7-R. The amplified DNA fragments were digested with *Sac*I and *Mlu*I, and inserted into the corresponding region of pUCp88-T7.

pBICp27-FLAG $Y_{207}A$, pBICp27-FLAG $Y_{207}F$, pBICp27-FLAG $RR_{214-215}AA$, pBICp27-FLAG $RR_{214-215}KK$, pBICp27-FLAG $R_{222}A$, pBICp27-FLAG $R_{222}K$, pBICp27-FLAG $F_{230}A$, and pBICp27-FLAG $F_{230}Y$

DNA fragments were amplified from pBICp27-iFLAG. The primer pairs used were BIC*Dra*III-F plus one each of the following: p27Y_{207}A-R, p27Y_{207}F-R, p27$RR_{214-215}$AA-R, p27$RR_{214-215}$KK-R, p27R_{222}A-R, p27R_{222}K-R, p27F_{230}A-R, and p27F_{230}Y-R. Another primer BIC*Hind*III-R was used together with one each of the following: p27Y_{207}A-F, p27Y_{207}F-F, p27$RR_{214-215}$AA-F, p27$RR_{214-215}$KK-F, p27R_{222}A-F, p27R_{222}K-F, p27F_{230}A-F, and p27F_{230}Y-F. Each recombinant PCR product was amplified using the primer pair, pBIC*Dra*III-F plus pBIC*Hind*III-R, digested with *Dra*III and *Hind*III, and inserted into the corresponding region of pBICp27-iFLAG.

pUCnGFP

DNA fragments were amplified from pBICGFP using the primer pair, nGFP-F plus T7-nGFP-R. The amplified DNA fragments were digested with *Hind*III and *Eco*RI, and inserted into pUC118 that had been cut with *Eco*RI and *Hind*III.

Expression and purification of His-p27-FLAG and its deletion mutants

E. coli strain BL21 (DE3) transformed by the plasmids with the prefix 'pCold' was grown overnight at 37 °C in Luria Broth (LB) medium containing ampicillin (50 μg/ml). The overnight culture (2 ml) of the transformed *E. coli* was added to 100 ml LB medium containing ampicillin (50 μg/ml). After incubation for 1.5 h at 37 °C and subsequent incubation for 30 min at 15 °C, protein expression was induced by the addition of 0.3 mM isopropyl-β-D-thiogalactopyranoside (IPTG). Cells were cultured at 15 °C for 24 h following induction. The induced cells were harvested at 5000×*g* for 5 min at 4 °C, resuspended in 1 ml of lysis buffer (20 mM Tris–HCl pH 8.0, 150 mM NaCl, and 30 mM imidazole), sonicated on ice to disrupt the cell. After sonication, Triton X-100 was added at the final concentration of 0.5% and centrifuged at 15,000×*g* for 10 min at 4 °C. The supernatant was added to the 50 μl bed volume of equilibrated Ni–NTA agarose (QIAGEN, Hilden, Germany) and incubated at 4 °C for 1 h with gentle rotation. The resin was washed three times with 1 ml of washing buffer (20 mM Tris–HCl pH 8.0, 150 mM NaCl, and 100 mM imidazole) and eluted with elution buffer (50 mM Tris–HCl pH7.4, 150 mM NaCl, 500 mM imidazole, 10% Glycerol, and 0.1% Triton X-100). The concentration of purified proteins was measured using Coomassie protein assay kit (Thermo Fisher Scientific, Waltham, MA, USA). The purified proteins were subjected to sodium dodecyl sulfate-PAGE (SDS — PAGE) and visualized with coomassie brilliant blue (CBB) R-250 to check their purity. If required, the purified proteins were analyzed by western blotting to confirm that equal amounts of them were used for GST pull-down assays.

GST pull-down assay

E. coli strain BL21 (DE3) transformed by the plasmids with the prefix 'pColdGST' was grown overnight at 37 °C in LB medium containing ampicillin (50 μg/ml). The overnight cultures of the transformed *E. coli* were diluted 1:50 in LB medium containing ampicillin (50 μg/ml). After incubation for 2.5 h at 37 °C and subsequent incubation for 30 min at 15 °C, protein expression was induced by addition of 0.3 mM IPTG. The cells expressing His/GST-p27, His/GST-p27N, or His/GST-p27C were cultured for 1 h. The cells expressing His/GST-p88 or His/GST-p88Δp27 were cultured for 4 h. The induced cells were harvested by centrifugation at 5000×*g* for 5 min.

Cells collected from 5 ml (His/GST, His/GST-p27, His/GST-p27N and His/GST-p27C) and 10 ml (His/GST-p88 and His/GST-p88Δp27) of medium were resuspended in 500 μl of phosphate buffer saline (140 mM NaCl, 2.7 mM KCl, 10 mM Na_2HPO_4, and 1.8 mM KH_2PO_4), and sonicated on ice to disrupt the cells. After sonication, Triton X-100 was added at the final concentration of 0.5% and centrifuged at 15,000×*g* for 10 min at 4 °C. The supernatant was added to 12.5 μl bed volume of equilibrated Glutathione Sepharose 4B (GE Healthcare, Little Chalfont, Buckinghamshire, UK), and incubated at 4 °C for 1 h with gentle rotation. The resin was washed three times with 1 ml of binding buffer (50 mM Tris–HCl pH 7.4, 150 mM NaCl, 10 mM 2-mercaptoethanol, and 0.5% Triton X-100). After washing, the resin was incubated for 2 h at 4 °C in 200 μl of binding buffer containing 500 ng of His-p27-FLAG or its deletion mutants. After incubation, the resin was washed four times with 1 ml of binding buffer. The bound proteins were eluted by addition of Laemmli sample buffer (Laemmli, 1970), followed by incubation for 3 min at 95 °C. Protein samples were subjected to SDS-PAGE and then blotted onto a PVDF membrane (Immobilon-P, Millipore, Bedford, MA, USA). The separated proteins were analyzed by western blotting using anti-FLAG M2 monoclonal antibody (Sigma-Aldrich, St. Louis, MO, USA) and horseradish peroxidase-conjugated anti-mouse IgG secondary antibody (KPL, Gaithersburg, MD, USA) as previously described (Okamoto et al., 2008). After detection, the separated proteins on the membrane were stained with PonceauS.

In vitro transcription

pRC2, pUCp27-FLAG, pUCp88-T7 and their derivatives were digested with *Sma*I, from which RNA transcripts were synthesized in the absence or presence of cap structure analog as described previously (Iwakawa et al., 2007, 2008).

Evacuolated BY-2 protoplast lysate (BYL) experiments

Preparation of the cell extracts of evacuolated BY-2 protoplasts was described previously (Komoda et al., 2004), and the *in vitro* translation/replication reactions were carried out essentially as described previously (Iwakawa et al., 2007). Briefly, capped transcripts of p27-FLAG or its derivatives (200 ng) together with capped transcripts of p88-T7 (100 ng) and RNA2 (500 ng) were added to each 50 μl BYL translation and replication mixture, followed by incubation at 17 °C for 4 h. Total proteins were analyzed by western blotting using anti-FLAG M2 monoclonal antibody or anti-T7 monoclonal antibody as previously described (Mine et al., 2010). Total RNAs were analyzed by northern blotting as previously described (Iwakawa et al., 2007).

In coimmunoprecipitation experiments, BYL was centrifuged at 21,000×*g* for 30 min at 4 °C to obtain the membrane fraction (P20). The P20 pellet was resuspended in 500 μl of resuspension buffer (Mine et al., 2010) and incubated on ice for 30 min. The resulting samples were incubated with 10 μl bed volume of anti-HA affinity matrix (Roche Diagnostics, Penzberg, Germany) or anti-T7 antibody agarose (Merck, Darmstadt, Germany) for 1 h at 4 °C with gentle

rotation. The resin was washed three times with 500 µl of resuspension buffer supplemented with 500 mM NaCl. The bound proteins were eluted by addition of Laemmli sample buffer, followed by incubation for 3 min at 95 °C. Protein samples were subjected to SDS-PAGE and then analyzed by western blotting with antibodies specific to respective epitope-tags as described previously (Mine et al., 2010).

BN-PAGE analysis was performed essentially as described previously (Mine et al., 2010). Briefly, the solubilized membrane fractions from BYL were subjected to BN — PAGE, followed by western blotting with anti-FLAG M2 monoclonal antibody.

Viral RNA replication and RNA silencing suppression assay

Viral RNA replication and RNA silencing suppression assay was performed as described previously (Takeda et al., 2005) with minor modification. The plasmids containing the prefix 'pBIC' were introduced into *Agrobacterium tumefaciens* GV3101 (pMP90) by electroporation. *Agrobacterium* suspensions prepared to OD_{600} of 0.8 were mixed and infiltrated into GFP-expressing *N. benthamiana* line 16c. At 4 dpi, total RNAs isolated from the *Agrobacterium*-infiltrated leaves were analyzed by northern blotting as described previously (Takeda et al., 2005), except that GFP mRNA and GFP-specific siRNAs were detected using digoxigenin-labeled RNA probe specific for sense GFP, which is transcribed from *Eco*RI-linearized pUCnGFP with T7 RNA polymerase. Protein samples prepared from the solubilized membrane fractions of *Agrobacterium*-infiltrated leaves were analyzed by western blotting after BN-PAGE and SDS-PAGE as described previously (Mine et al., 2010).

Acknowledgments

The authors thank S. A. Lommel for the original RNA1 and RNA2 cDNA clones of RCNMV Australian strain, and D. C. Baulcombe for *Nicotiana benthamiana* line 16C. The authors are also grateful to H. Iwakawa for helpful discussion. This work was supported in part by a Grant-in-Aid for Scientific Research (A) (18208004) and by a Grant-in-Aid for Scientific Research (A) (22248002) from the Japan Society for the Promotion of Science.

Appendix A. Supplementary data

Supplementary data associated with this article can be found, in the online version, at doi:10.1016/j.virol.2010.07.038.

References

Ahlquist, P., Noueiry, A.O., Lee, W.M., Kushner, D.B., Dye, B.T., 2003. Host factors in positive-strand RNA virus genome replication. J. Virol. 77, 8181–8186.
Bates, H.J., Farjah, M., Osman, T.A.M., Buck, K.W., 1995. Isolation and characterization of an RNA-dependent RNA polymerase from *Nicotiana clevelandii* plants infected with red clover necrotic mosaic dianthovirus. J. Gen. Virol. 76, 1483–1491.
Daugherty, M.D., D'Orso, I., Frankel, A.D., 2008. A solution to limited genomic capacity: using adaptable binding surfaces to assemble the functional HIV Rev oligomer on RNA. Mol. Cell 31, 824–834.
Dye, B.T., Miller, D.J., Ahlquist, P., 2005. In vivo self-interaction of Nodavirus RNA replicase protein A revealed by fluorescence resonance energy transfer. J. Virol. 79, 8909–8919.
Goregaoker, S.P., Culver, J.N., 2003. Oligomerization and activity of the helicase domain of the tobacco mosaic virus 126- and 183-kilodalton replicase proteins. J. Virol. 77, 3549–3556.
Goregaoker, S.P., Lewandowski, D.J., Culver, J.N., 2001. Identification and functional analysis of an interaction between domains of the 126/183-kDa replicase-associated proteins of tobacco mosaic virus. Virology 282, 320–328.
Hobson, S.D., Rosenblum, E.S., Richards, O.C., Richmond, K., Kirkegaard, K., Schultz, S.C., 2001. Oligomeric structures of poliovirus polymerase are important for function. EMBO J. 20, 1153–1163.
Hope, D.A., Diamond, S.E., Kirkegaard, K., 1997. Genetic dissection of interaction between poliovirus 3D polymerase and viral protein 3AB. J. Virol. 71, 9490–9498.
Iwakawa, H.O., Kaido, M., Mise, K., Okuno, T., 2007. *cis*-Acting core RNA elements required for negative-strand RNA synthesis and cap-independent translation are separated in the 3′-untranslated region of red clover necrotic mosaic virus RNA1. Virology 369, 168–181.
Iwakawa, H.O., Mizumoto, H., Nagano, H., Imoto, Y., Takigawa, K., Sarawaneeyaruk, S., Kaido, M., Mise, K., Okuno, T., 2008. A viral noncoding RNA generated by *cis*-element-mediated protection against 5′->3′ RNA decay represses both cap-independent and cap-dependent translation. J. Virol. 82, 10162–10174.
Kadare, G., Haenni, A.L., 1997. Virus-encoded RNA helicases. J. Virol. 71, 2583–2590.
Kao, C.C., Ahlquist, P., 1992. Identification of the domains required for direct interaction of the helicase-like and polymerase-like RNA replication proteins of brome mosaic virus. J. Virol. 66, 7293–7302.
Kao, C.C., Quadt, R., Hershberger, R.P., Ahlquist, P., 1992. Brome mosaic virus RNA replication proteins 1a and 2a form a complex in vitro. J. Virol. 66, 6322–6329.
Kim, K.H., Lommel, S.A., 1994. Identification and analysis of the site of −1 ribosomal frameshifting in red clover necrotic mosaic virus. Virology 200, 574–582.
Komoda, K., Naito, S., Ishikawa, M., 2004. Replication of plant RNA virus genomes in a cell-free extract of evacuolated plant protoplasts. Proc. Natl. Acad. Sci. U. S. A. 101, 1863–1867.
Koonin, E.V., 1991. The phylogeny of RNA-dependent RNA polymerases of positive-strand RNA viruses. J. Gen. Virol. 72, 2197–2206.
Koonin, E.V., Dolja, V.V., 1993. Evolution and taxonomy of positive strand RNA viruses: implications of comparative analysis of amino acid sequences. Crit. Rev. Biochem. Mol. Biol. 28, 375–430.
Laemmli, U.K., 1970. Cleavage of structural proteins during the assembly of the head of bacteriophage T4. Nature 227, 680–685.
Lommel, S.A., Westonfina, M., Xiong, Z., Lomonossoff, G.P., 1988. The nucleotide sequence and gene organization of red clover necrotic mosaic virus RNA-2. Nucleic Acids Res. 16, 8587–8602.
Ma, B.Y., Elkayam, T., Wolfson, H., Nussinov, R., 2003. Protein–protein interactions: structurally conserved residues distinguish between binding sites and exposed protein surfaces. Proc. Natl. Acad. Sci. U. S. A. 100, 5772–5777.
Mine, A., Takeda, A., Taniguchi, T., Taniguchi, H., Kaido, M., Mise, K., Okuno, T., 2010. Identification and characterization of the 480-kilodalton template-specific RNA-dependent RNA polymerase complex of red clover necrotic mosaic virus. J. Virol. 84, 6070–6081.
Mizumoto, H., Tatsuta, M., Kaido, M., Mise, K., Okuno, T., 2003. Cap-independent translational enhancement by the 3′ untranslated region of red clover necrotic mosaic virus RNA1. J. Virol. 77, 12113–12121.
Mizumoto, H., Iwakawa, H.O., Kaido, M., Mise, K., Okuno, T., 2006. Cap-independent translation mechanism of red clover necrotic mosaic virus RNA2 differs from that of RNA1 and is linked to RNA replication. J. Virol. 80, 3781–3791.
O'Reilly, E.K., Tang, N.J., Ahlquist, P., Kao, C.C., 1995. Biochemical and genetic analyses of the interaction between the helicase-like and polymerase-like proteins of the brome mosaic virus. Virology 214, 59–71.
O'Reilly, E.K., Paul, J.D., Kao, C.C., 1997. Analysis of the interaction of viral RNA replication proteins by using the yeast two-hybrid assay. J. Virol. 71, 7526–7532.
O'Reilly, E.K., Wang, Z.H., French, R., Kao, C.C., 1998. Interactions between the structural domains of the RNA replication proteins of plant-infecting RNA viruses. J. Virol. 72, 7160–7169.
Okamoto, K., Nagano, H., Iwakawa, H., Mizumoto, H., Takeda, A., Kaido, M., Mise, K., Okuno, T., 2008. *cis*-Preferential requirement of a −1 frameshift product p88 for the replication of Red clover necrotic mosaic virus RNA1. Virology 375, 205–212.
Patel, S.S., Picha, K.M., 2000. Structure and function of hexameric helicases. Annu. Rev. Biochem. 69, 651–697.
Pogany, J., White, K.A., Nagy, P.D., 2005. Specific binding of tombusvirus replication protein p33 to an internal replication element in the viral RNA is essential for replication. J. Virol. 79, 4859–4869.
Qin, W.P., Luo, H., Nomura, T., Hayashi, N., Yamashita, T., Murakami, S., 2002. Oligomeric interaction of hepatitis C virus NS5B is critical for catalytic activity of RNA-dependent RNA polymerase. J. Biol. Chem. 277, 2132–2137.
Rajendran, K.S., Nagy, P.D., 2004. Interaction between the replicase proteins of Tomato Bushy Stunt Virus in vitro and in vivo. Virology 326, 250–261.
Rajendran, K.S., Nagy, P.D., 2006. Kinetics and functional studies on interaction between the replicase proteins of Tomato Bushy Stunt Virus: requirement of p33: p92 interaction for replicase assembly. Virology 345, 270–279.
Strauss, D.M., Wuttke, D.S., 2007. Characterization of protein–protein interactions critical for poliovirus replication: analysis of 3AB and VPg binding to the RNA-dependent RNA polymerase. J. Virol. 81, 6369–6378.
Takeda, A., Tsukuda, M., Mizumoto, H., Okamoto, K., Kaido, M., Mise, K., Okuno, T., 2005. A plant RNA virus suppresses RNA silencing through viral RNA replication. EMBO J. 24, 3147–3157.
Turner, K.A., Sit, T.L., Callaway, A.S., Allen, N.S., Lommel, S.A., 2004. Red clover necrotic mosaic virus replication proteins accumulate at the endoplasmic reticulum. Virology 320, 276–290.
Wang, Q.M., Hockman, M.A., Staschke, K., Johnson, R.B., Case, K.A., Lu, J.R., Parsons, S., Zhang, F.M., Rathnachalam, R., Kirkegaard, K., Colacino, J.M., 2002. Oligomerization and cooperative RNA synthesis activity of hepatitis C virus RNA-dependent RNA polymerase. J. Virol. 76, 3865–3872.
Watanabe, T., Honda, A., Iwata, A., Ueda, S., Hibi, T., Ishihama, A., 1999. Isolation from tobacco mosaic virus-infected tobacco of a solubilized template-specific RNA-dependent RNA polymerase containing a 126K/183K protein heterodimer. J. Virol. 73, 2633–2640.
Xiong, Z., Lommel, S.A., 1989. The complete nucleotide sequence and genome organization of red clover necrotic mosaic virus RNA-1. Virology 171, 543–554.
Xiong, Z.G., Lommel, S.A., 1991. Red clover necrotic mosaic virus infectious transcripts synthesized *in vitro*. Virology 182, 388–392.
Xiong, Z., Kim, K.H., Kendall, T.L., Lommel, S.A., 1993. Synthesis of the putative red clover necrotic mosaic virus RNA polymerase by ribosomal frameshifting in vitro. Virology 193, 213–221.